Carbohydrate Polymers 94 (2013) 850–856

Contents lists available at SciVerse ScienceDirect

Carbohydrate Polymers

journal homepage: www.elsevier.com/locate/carbpol

Doxorubicin loading fucoidan acetate nanoparticles for immune and chemotherapy in cancer treatment

Kun Woo Lee[a,1], Dooyong Jeong[b,1], Kun Na[b,*]

[a] Biotechnology, Department of Life Science, Korea University, Anam-ro 145, Sungbuk-gu, Seoul 136-701, Republic of Korea
[b] Department of Biotechnology, The Catholic University of Korea, 43 Jibong-ro, Wonmi-gu, Bucheon-si, Gyeonggi-do 420-743, Republic of Korea

ARTICLE INFO

Article history:
Received 7 January 2013
Received in revised form 11 February 2013
Accepted 13 February 2013
Available online 20 February 2013

Keywords:
Immuno-chemotherapy
Acetylated fucoidan
Anti-tumor cytokines
Multidrug resistance

ABSTRACT

In order to develop immuno- and chemotherapy agents, self-organized acetylated fucoidan (AcFu) nanoparticles were designed. Doxorubicin (DOX), used as a model drug, was loaded into the AcFu nanoparticles by dialysis. The DOX loading efficacy and content were 71.1% and 3.6%, respectively. Approximately 140 nm of spherical nanoparticles were obtained. DOX-loaded AcFu nanoparticles (DOX–AcFu) exhibited first-order drug release behavior for 5 days. Interestingly, AcFu treated Raw264.7 macrophages overexpressed various anti-tumor cytokines, such as tumor necrosis factor-alpha (TNF-α) and granulocyte-macrophage colony-stimulating factor (GM-CSF). The ability of DOX–AcFu to suppress drug efflux was revealed by confocal microscope images and FACS analysis in multidrug resistance (MDR) cells. IC_{50} (50% inhibitory concentration) value of DOX–AcFu was lower than that of free DOX in the MDR model cells. Based on these results, we strongly suggest that AcFu nanoparticles have a promising potential for development as a one-step therapy containing agents for both immuno- and chemotherapy.

1. Introduction

Previously, two different therapeutic methods have been developed for cancer patients. The first is chemotherapy: treatment with chemotherapeutic agents (Wagner et al., 2006). The other method, immunotherapy, involves enhancing an immune response against cancer (Rosenberg, Yang, & Restifo, 2004). Despite considerable research for several decades regarding these separate therapeutic systems, some impassable hurdles still exist. Chemotherapy has several disadvantages, including the numerous side effects and low cellular uptake efficiency of chemotherapeutic agents caused by the multidrug resistance (MDR) property of cancer cells. Furthermore, the curative efficiency of immunotherapy for cancer is limited by the complexities of cancer cells and a short period of activity due to the host's immune tolerance (Perales et al., 2002).

Here, we suggest a new concept for immuno-chemotherapy. According to the notable report of a clinical trial conducted by Rosenberg and colleagues, the combination of chemotherapy and immunotherapy produced strong clinical responses in 18 out of 35 patients (van der Most, Robinson, & Lake, 2009). However, the relative timing of the chemotherapy and immunotherapy is crucial. Specifically, if the immunotherapy is delayed following chemotherapy, all benefits disappear (Lake & Robinson, 2005). Therefore, we assumed that a combination of immunotherapy and chemotherapy in a single system may provide a more efficient treatment method.

In this study, fucoidan was used as an immuno-therapeutic functional polymer. Xun Qu et al. have studied the immunomodulatory functions of fucoidan, which induces the maturation of human monocyte-derived dendritic cells (Yang et al., 2008). Additionally, J.K. Hang's group reported that fucoidan stimulates the activation of lymphocytes and macrophages (Choi, Kim, Kim, & Hwang, 2005). In another study, Masahiro Kizaki concluded that the fucoidan-induced enhancement of immune responses is involved in the anti-cancer effects of fucoidan (Aisa et al., 2005). Furthermore, fucoidan has ability to inhibit the p-glycoprotein mediated drug efflux system (Bernkop-Schnurch & Grabovac, 2006).

Therefore, we designed fucoidan-based nanoparticles for delivery of combined immuno-chemotherapy (Fig. 1A). To prepare the chemotherapeutic agent-loaded nanoparticles, hydrophobically modified fucoidan was synthesized by acetylation of fucoidan (Fig. 1B).

Doxorubicin (DOX) was used as a model chemotherapeutic agent, and the drug was loaded in the acetylated fucoidan (AcFu) nanoparticles. The nanoparticles were simply characterized by their morphology and drug release properties. In addition, the improved cellular internalization efficiency and immuno-chemotherapeutic effects of the nanoparticles were investigated using in vitro studies.

* Corresponding author. Tel.: +82 2 2164 4832; fax: +82 2 2164 4865.
E-mail address: kna6997@catholic.ac.kr (K. Na).
[1] These authors were equally contributed to this paper.

0144-8617/$ – see front matter © 2013 Elsevier Ltd. All rights reserved.
http://dx.doi.org/10.1016/j.carbpol.2013.02.018

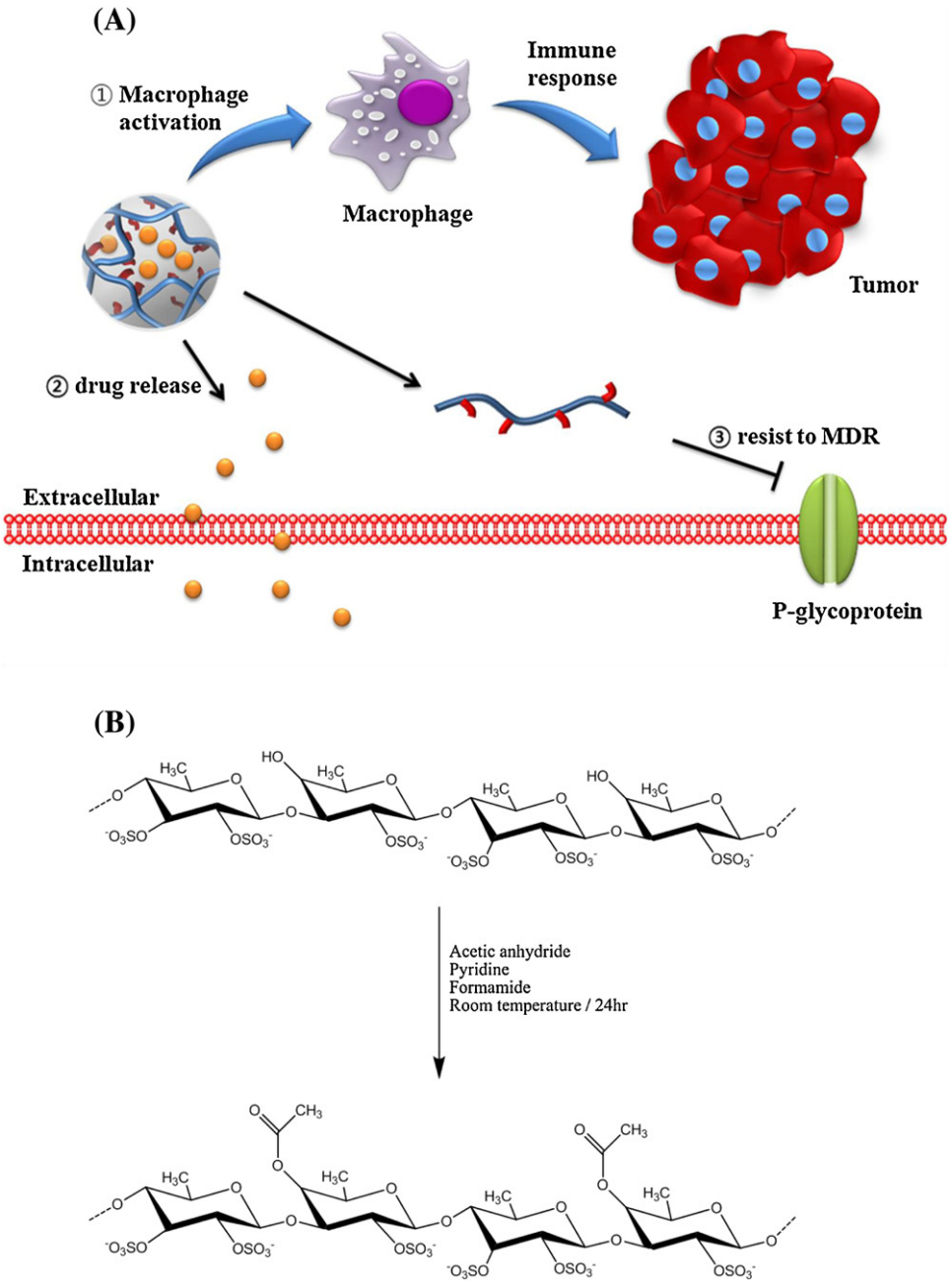

Fig. 1. (A) Schematic illustration of anticancer mechanism of drug-loaded AcFu nanoparticles. (B) Synthesis method and chemical structure of AcFu.

2. Materials and methods

2.1. Materials

Fucoidan from *Fucus vesiculosus* was purchased from Sigma Aldrich. DOX·HCl was purchased from ILDONG Pharm. Co., HCT-8 and HCT-116 were obtained from the Korea Cell Bank (Seoul, Korea). Pyridine, acetic anhydride and other reagents were purchased from Junsei Chemical (Tokyo, Japan) and were used without further purification.

2.2. Synthesis of acetylated fucoidan

Acetylated fucoidan (AcFu) was obtained using our previously described methods (Li, Bae, & Na, 2010; Park, Park, & Na, 2010). Briefly, 1 g of fucoidan was dissolved in 10 mL of formamide, followed by addition of 1 mL of pyridine and 3 mL of acetic anhydride to the fucoidan solution. After 24 h, the reactant was purified by dialysis for 3 days, and then freeze dried. The structure and acetylation degree of AcFu was determined by ^{1}H NMR and FT-IR. In addition, the hydrophobicity of AcFu was examined by measuring the critical aggregation concentration (CAC), which was described in our previous report (Park, Kim, Bae, Kim, & Na, 2010) and supporting data.

2.3. Preparation of doxorubicin loaded AcFu nanoparticles

DOX·HCl (5 mg) was dissolved in 10 mL of anhydrous DMSO containing 6.2 μL of triethylamine (TEA) for 12 h at room temperature. After adding 100 mg of AcFu into the DOX solution, the mixture was stirred overnight and then dialyzed against deionized water for

12 h. The dialysates were kept at −20 °C until required for further experiments.

To determine the drug loading efficiency and drug contents, samples were freeze-dried and then dissolved in DMSO. The amount of DOX was quantified by UV spectrophotometry at 490 nm. Finally, these two parameters were calculated by following equations:

$$\text{Drug loading efficiency} = \frac{\text{amount of drug in nanoparticles}}{\text{amount of drug initially added}} \times 100 \quad \text{(A.1)}$$

$$\text{Drug contents} = \frac{\text{amount of drug}}{\text{amount of drug and polymer}} \times 100 \quad \text{(A.2)}$$

2.4. Morphological characterization of DOX loaded AcFu nanoparticles

The hydrodynamic size of the DOX loaded nanoparticles was measured using a dynamic light scattering (DLS) system (Nanosizer, Malvern). The autocorrelation intensity was measured at a scattering angle (θ) of 90° at 25 °C. All samples were measured in triplicate, and the results were averaged. In addition, a field emission scanning electron microscopy (FE-SEM, S4800, Hitachi) was used to confirm the morphology of the DOX-loaded AcFu nanoparticles. To prepare the SEM samples, a 10 μL aliquot of the nanoparticle solution was dropped on a cover glass and dried for 12 h. Then, it was coated with platinum (15 mA, 45 s).

2.5. In vitro drug release

1 mL of the DOX-loaded AcFu nanoparticle solution was dialyzed against 10 mL of phosphate buffered saline solution (PBS, pH 7.4) using a cellulose acetate membrane (Spectra, MWCO: 1000 Da) in a shaking water bath (50 rpm, 37 °C). At the designated time interval, all of the outer solution was exchanged for fresh PBS solution, and the solution containing the released DOX was used for quantitative analysis. The absorbance of the released DOX was measured at 490 nm by UV/vis spectrophotometry.

2.6. Cell culture

HCT-116 and HCT-8 cells were cultured in RPMI-1640 medium (GIBCO, Grand Island, NY) equilibrated with a 5% CO_2 atmosphere at 37 °C. The medium was supplemented with 10% fetal bovine serum (FBS) and 0.1% antibiotics.

2.7. Immunomodulatory activities of AcFu nanoparticles

The expression of TNF-α and GM-CSF was evaluated to determine the immunomodulatory activities of AcFu. Raw264.7 macrophage cells were plated at 1×10^5 cells/well in a 6-well plate with Dulbecco's modified Eagle's medium (DMEM, GIBCO, Grand Island, NY) containing 10% FBS and 0.1% antibiotics. After 1 day, the medium was changed to serum-free medium, and the cells were then incubated with 10 μg of fucoidan or acetylated fucoidan for 24 h. Finally, each of released cytokines in the medium was measured using ELISA kits (eBioscience, San Diego, CA). The results were statistically analyzed using Student's *t*-test, $n = 3$.

2.8. Cellular uptake of DOX

The cellular uptake of DOX provided in nanoparticles compared with that of free DOX was detected by fluorescence-activated cell sorting (FACS) analysis using the intrinsic fluorescence of doxorubicin (FL3). HCT-116 and HCT-8 cells were plated at 1×10^5 cells/well in a 6-well plate and then incubated with each type of sample (containing 1 μg/mL of DOX) under the standard condition (5% CO_2, 37 °C). After the designated incubation times (0, 0.5, 1, 2, 4 h), the cells were washed twice with PBS solution (pH 7.4) and then evaluated using a FACSCalibur flow cytometer (Becton Dickinson, San Jose, CA, USA).

The cellular uptake of DOX was also visualized by confocal microscopy. HCT-8 cells were grown on sterilized cover glasses at a density of 2×10^5. The cells were pre-incubated for 6 h under the standard condition in the serum-free RPMI 1640 medium. DOX-loaded AcFu nanoparticles or free DOX solutions were added to the wells. After 4 h, the medium was removed, and the cells were washed three times with DPBS. Then, they were fixed with 4% paraformaldehyde for 10 min. The nuclei were stained with 1 μL of 4,6-diamidino-2-phenylindole (DAPI). After washing, the cover glasses were mounted in medium for fluorescence evaluation (Dako, Glostrup, Denmark). DOX fluorescence was monitored in RITC channel, and randomly selected images were obtained using a confocal laser scanning microscope (Zeiss, LSM 510 Meta, Germany). For the HCT-116 cells, a non-MDR colon cancer cell line, the uptake was simply observed by fluorescence microscopy.

2.9. Cytotoxicity against MDR cancer cells

The cytotoxicity of the AcFu nanoparticles was determined using the MTT (3-(4,5-dimethyl-2-thiazolyl)-2,5-diphenyl-2H-tetrazolium bromide) assay. Briefly, 1×10^4 of HCT-116 and HCT-8 cells were grown in 96-well plates in RPMI 1640 medium supplemented with 10% FBS and 0.1% antibiotics. On the days of the experiments, the cells were incubated for a total of 48 h with various concentrations of DOX-loaded AcFu nanoparticles or free DOX. The cell viability was assessed colorimetrically with the MTT reagent at 570 nm. The control cells were incubated without either form of DOX.

3. Results

3.1. Synthesis of AcFu

AcFu was synthesized by pyridine-mediated addition-elimination mechanism. In the ^{1}H NMR data (Fig. 2A), the peaks between 1.86 and 2.49 ppm indicate the three hydrogens of the methyl of the O-acetyl group. On each fucose molecule, 0.87 of the hydroxyl groups were substituted with acetyl groups. The details of the ^{1}H NMR peaks are described as follows: 0.99–1.66 ppm: CH_3 (C_6 in fucose), 1.86–2.49 ppm: CH (acetyl group), 3.8–3.95 ppm: OH (C_3 in fucose), 4.11–5.77 ppm: CH of fucose, 4.82 ppm: D_2O.

In the FT-IR data (Fig. 2B), peaks at 1730 cm^{-1} for C=O, 1370 cm^{-1} for CH_3 of acetyl group, and 1230 cm^{-1}: C—O for ester bond were observed in AcFu but not in natural fucoidan. The peaks of the hydroxyl groups (3600–3200 cm^{-1}) were also reduced from those of the natural fucoidan.

Finally, the CAC of AcFu was estimated to be 0.039 ± 0.002 mg/mL, whereas that of the natural fucoidan was 0.426 ± 0.003 mg/mL.

3.2. Formation of DOX-loaded AcFu nanoparticles

DOX was loaded into AcFu nanoparticles via dialysis. The drug contents and loading efficiency were 3.6% and 71.1%, respectively. The hydrodynamic diameter of the DOX loaded nanoparticles was 137.5 ± 2.475 nm as measured by DLS (Fig. 3A). The Pdi value of the diameter was 0.231 ± 0.013, and the correlation peak was monodisperse (Table 1). In the SEM images, spherical DOX-loaded AcFu nanoparticles were observed (Fig. 3B).

Table 1
Characterization of AcFu nanoparticle.

Sample	Degree of acetylation[a]	CAC[b] (mg/mL)	Drug loading efficiency (%)	Drug contents (%)	Hydrodynamic diameter (nm)	Pdi value[c]
DOX loaded AcFu nanoparticle	0.870 ± 0.005	0.039 ± 0.002	71.1 ± 1.3	3.6 ± 0.3	137.5 ± 2.475	0.231 ± 0.013

[a] Substitution ratio of acetyl group against total hydroxyl residue.
[b] Critical aggregation concentration of AcFu (Fig. S1).
[c] Polydispersity index of hydrodynamic diameter.

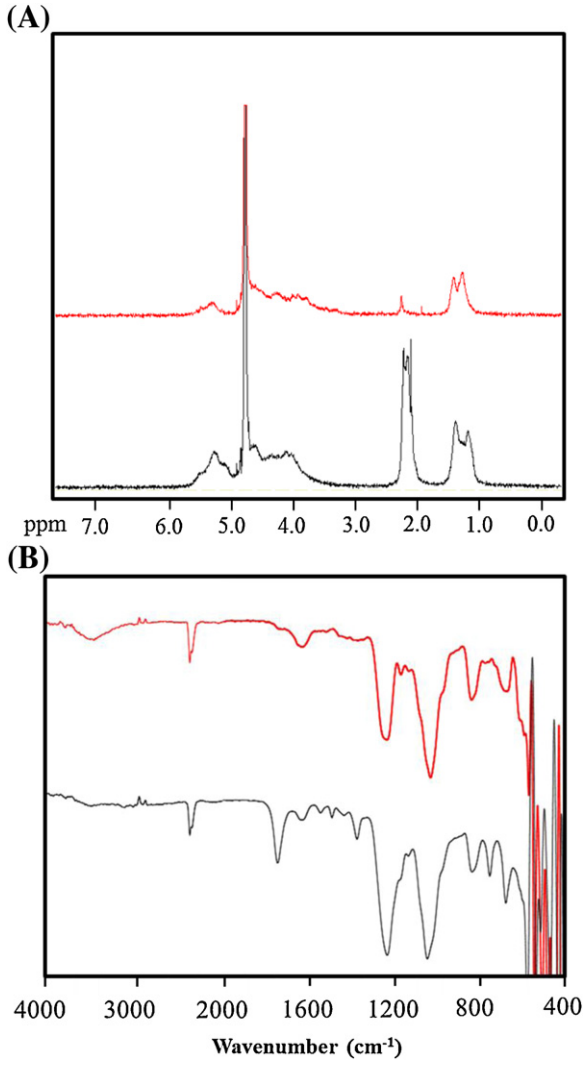

Fig. 2. Structural characterization of AcFu. (A) ^{1}H NMR and (B) FT-IR are shown for natural fucoidan (red line, upper line) and AcFu (black line, lower line). (For interpretation of the references to color in this figure legend, the reader is referred to the web version of the article.)

3.3. Drug release

DOX was released from AcFu by first-order kinetics (Fig. 4A and B). The half-life time for DOX release was 19.2 h. Therefore, the total release time was approximately 120 h. The release of DOX from 1 mL of the DOX-loaded AcFu nanoparticle solution during the first half-life was 17.7 μg of DOX. The following equation describes the drug release:

$$\text{Accumulated drug release rate } (\%) = 58.199 \times \log T - 24.709 \quad \text{(B.1)}$$

where T is the time (h) since the beginning of the drug release.

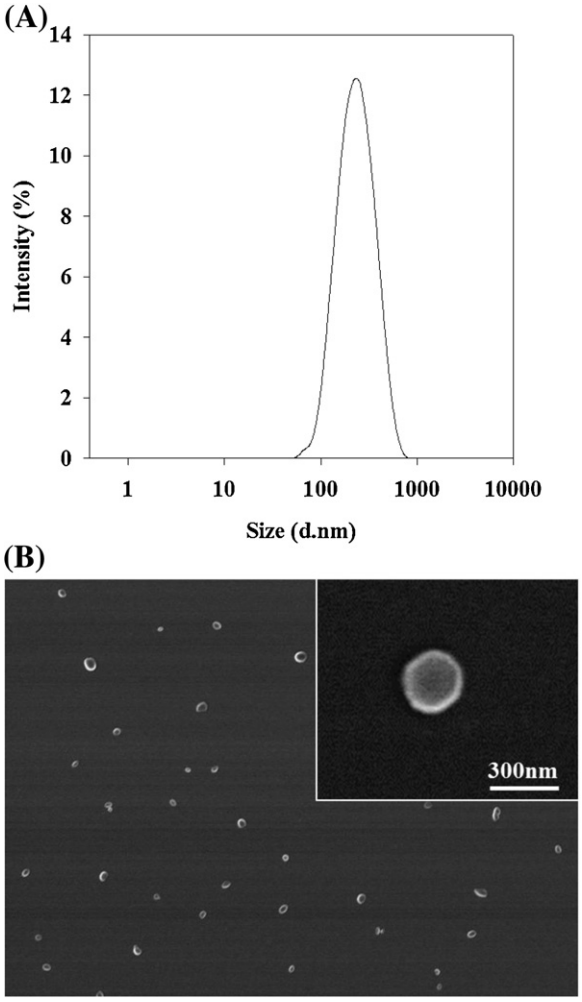

Fig. 3. Morphological characteristic of DOX loaded AcFu nanoparticle. (A) Size distribution graph of DOX-loaded AcFu nanoparticles, determined by dynamic light scattering. (B) Scanning electron microscopic images of AcFu nanoparticles.

3.4. Immunomodulatory activity

The expression levels of two immune-related cytokines, TNF-α and GM-CSF, were measured to determine the immunomodulatory activity of AcFu nanoparticles. When Raw264.7 macrophage cells were treated with 10 μg of AcFu, the TNF-α levels were increased by a factor of 1.13 (Fig. 5A), while GM-CSF was increased 1.86-fold (Fig. 5B) relative to the non-treated cells (negative control). These immunomodulatory effects of AcFu were similar to those of the natural fucoidan (positive control).

3.5. Cellular internalization efficiency

In the HCT-8 cells (MDR model cells), time-dependent cellular internalization of drug was observed in the case of DOX-loaded AcFu nanoparticles. After 2 h, over the 99% of the total DOX

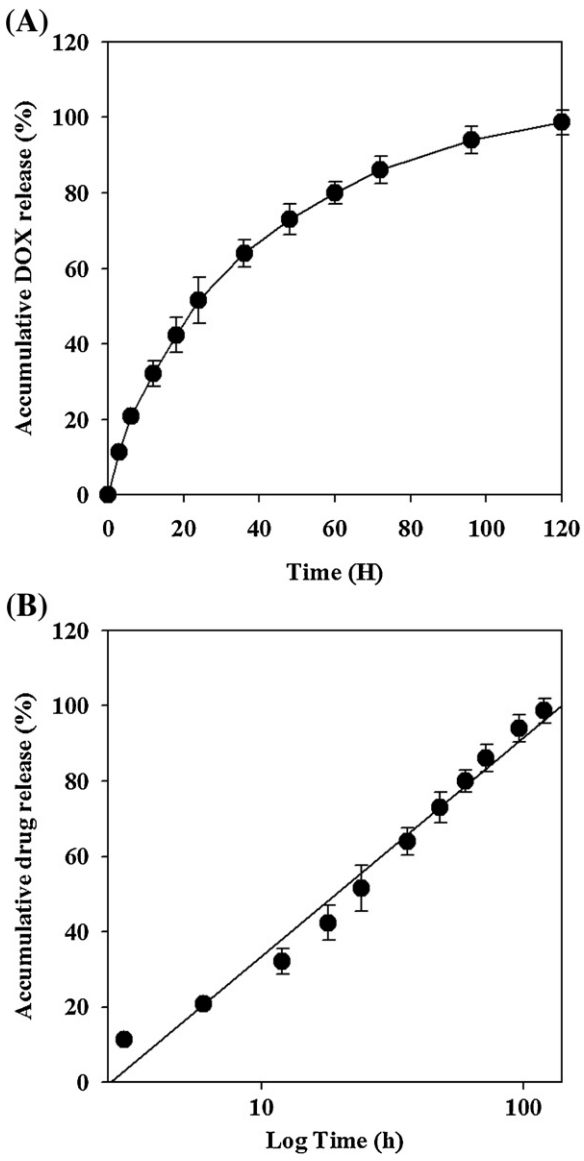

Fig. 4. Drug release behavior of AcFu nanoparticle. The model drug (DOX) was released from AcFu nanoparticle. (A) Time-dependent drug release was shown for AcFu nanoparticles with (B) first-order drug release behavior.

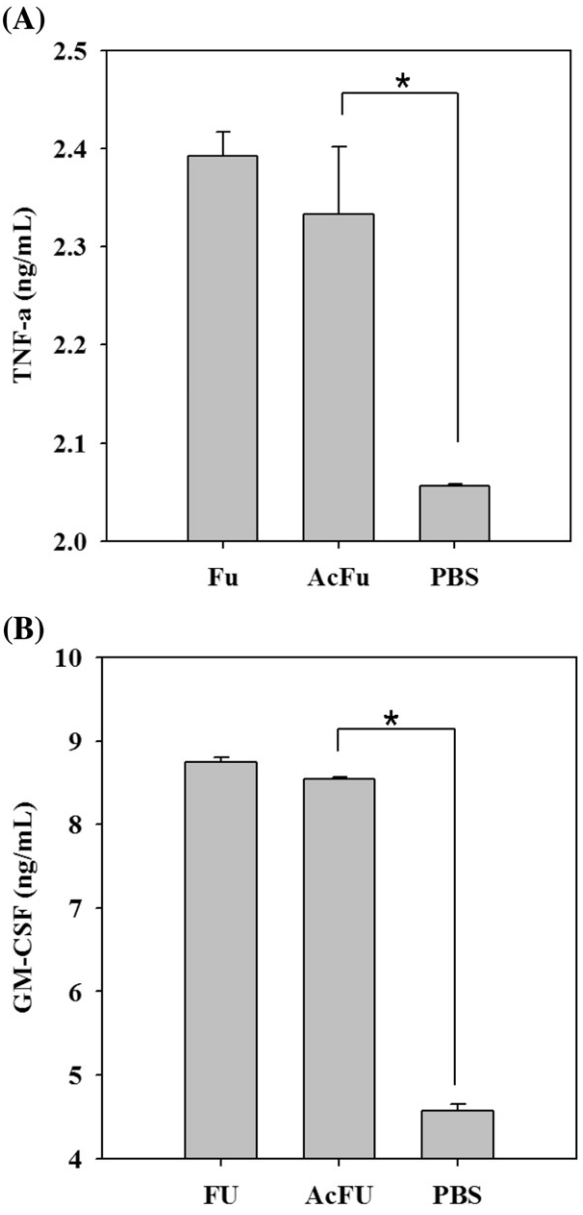

Fig. 5. Immunomodulatory activity of AcFu nanoparticle. The cancer immunotherapy-related cytokines (A) TNF-α and (B) GM-CSF were stimulated by AcFu in Raw264.7 macrophages. The immunomodulatory activity of AcFu was similar to that of natural fucoidan. The data were statistically analyzed by student's *t*-test ($^*p < 0.05$, $n = 3$).

was internalized into HCT-8 cells whereas 1.99% and 1.79% for fucoidan–DOX mixture and free DOX, respectively, were internalized (Fig. 6A–D). The internalized DOX was not released to the extracellular space even at 4 h. Only the DOX-loaded AcFu nanoparticles were clearly identified in the confocal images (Fig. 6E).

In the HCT-116 cells (non-MDR cells), cellular uptake of free DOX was similar to that of the AcFu nanoparticle-encapsulated DOX (Fig. 6F).

3.6. Cytotoxicity against cancer cell

In the cancer cells without increased drug efflux characteristics (HCT-116), the cytotoxicity of the DOX in AcFu nanoparticle was similar to that of the free drug: the IC_{50} (50% inhibitory concentration) values were ~1 μg/mL (Fig. 7A). However, in the case of the MDR cells (HCT-8), the free drug was 23.9-fold times less cytotoxic than in the HCT-116 cells, whereas the toxicity of AcFu-encapsulated DOX was similar for the two cell types (Fig. 7B).

4. Discussion

To develop a one-step immuno-chemotherapeutic system, hydrophobically modified fucoidan was synthesized. On the basis of the C_4-sulfated fucose structure, 87% of hydroxyl residues were modified with the hydrophobic acetyl group (Fig. 2). Consequently, the AcFu had approximately ten times lower CAC values (0.035 mg/mL) than the natural fucoidan (0.316 mg/mL) (Table 1). Thus, we used these particles to produce the hydrophobic drug-loaded nanoparticles. In our results, 137.52 nm diameter spherical nanoparticles (Fig. 3) were formed with 71.1% of drug loading efficiency and 3.6% drug contents (Table 1).

Interestingly, the DOX-loaded AcFu nanoparticles showed first-order drug release kinetic (Fig. 4). According to the general one-compartment drug elimination model (Chen, Lee, Li, & Yang, 1997; Grochow et al., 1989), the AcFu nanoparticles may be used

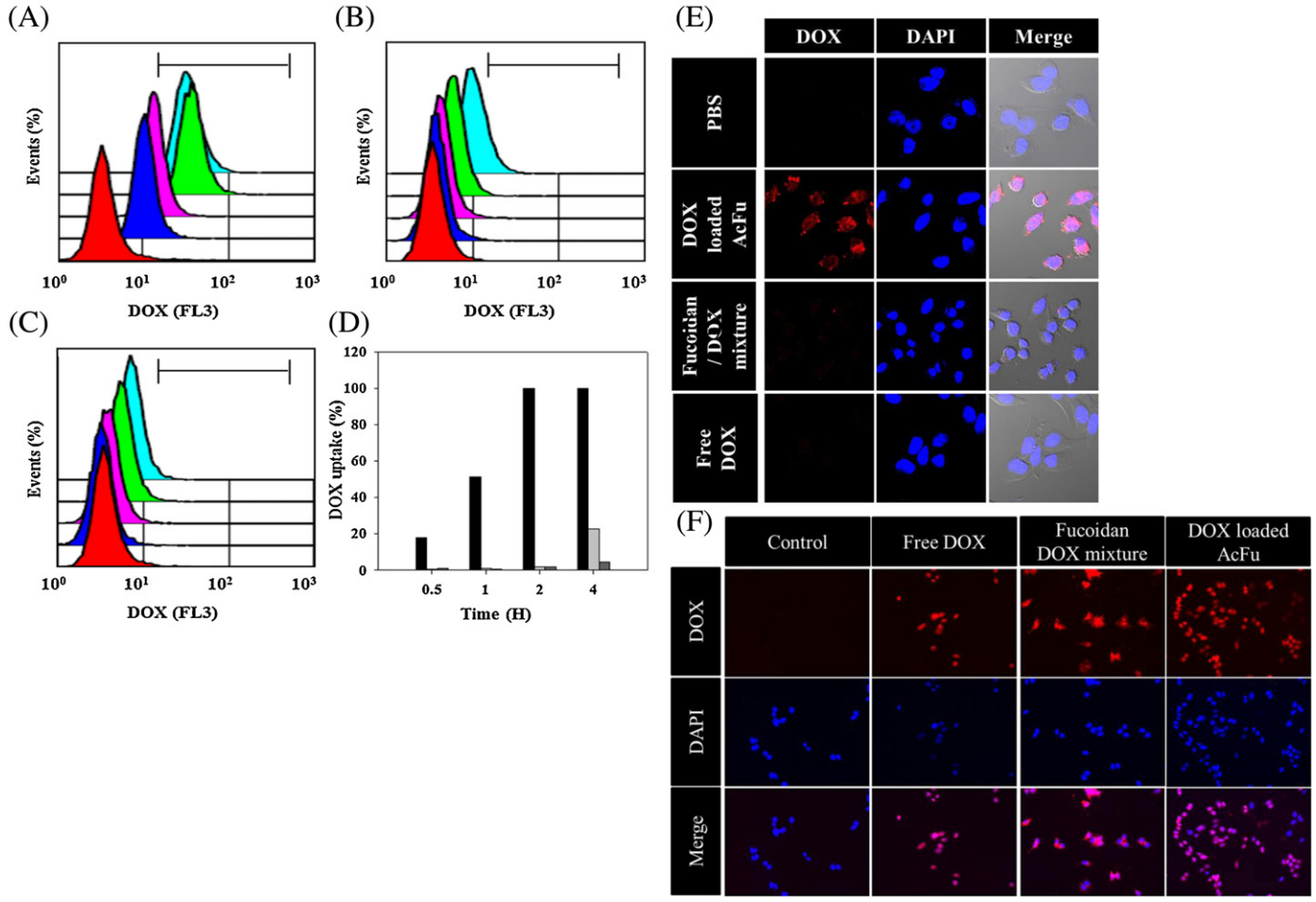

Fig. 6. Cellular uptake of DOX in the HCT-8 multidrug resistant (MDR) cell line. The time-dependent cellular uptake efficiency of DOX was estimated by FACS analysis. (A) DOX-loaded AcFu nanoparticles, (B) natural fucoidan–DOX mixtures, (C) free DOX. The colors in these graphs indicate the time after sample treatment: red – control; blue – 30 min; pink – 1 h; green – 2 h; sky blue – 4 h after sample treatment. The uptake efficiencies at each time points are indicated as a bar graph in (D). (Black: DOX loaded AcFu nanoparticle; gray: natural fucoidan–DOX mixture; dark gray: free DOX.) In addition, confocal images of DOX uptake after 4 h of treatment were shown (E). After 4 h sample treatment, cellular uptake of DOX in HCT-116 cells (F). (For interpretation of the references to color in this figure legend, the reader is referred to the web version of the article.)

to maintain a uniform plasma drug concentration, similar to a continuous infusion. Nevertheless, some factors such as the solubility of the drug, volume of distribution and drug elimination constant, must still be considered in the context of direct clinical application. We expect that these factors may be controlled via the degree of acetylation of AcFu. With respect to these issues, other studies of controlled-release drug delivery carriers reveal that the in vitro hydrophobic drug loading and release behaviors of amphiphilic polymer-based micellar systems are strongly affected by hydrophobic properties of the polymer (Jeong, Seo, & Na, 2012; Kim, Shin, Lee, Cho, & Sung, 1998).

The AcFu has another important function, the induction of immune reactions against cancer. In the previous studies, natural fucoidan has demonstrated immunotherapeutic effects for cancer because it induces production of some anticancer cytokines by macrophages (Choi et al., 2005; Maruyama, Tamauchi, Hashimoto, & Nakano, 2003). Two of these cytokines, TNF-α and GM-CSF, have crucial roles in cancer immunotherapy. TNF-α is required for natural killer (NK) cells, lymphokine-activated killer (LAK) cells, and dendritic cells to induce tumor killing and rejection (Baxevanis et al., 2000; Manna & Mohanakumar, 2002). Furthermore, a number of studies have examined the synergistic effects of TNF in combination with chemotherapy agents (Waterston & Bower, 2004). Similarly, GM-CSF generates mature $CD8^+$, $CD11b^+$ dendritic cells that effectively capture dying cancer cells and stimulate a coordinated humoral and cellular immune response. Our results show that AcFu has immunomodulatory activities similar to those of natural fucoidan, including induction of TNF-α (Fig. 5A) and GM-CSF (Fig. 5B). Based on these data, we suggest that AcFu has potential for use as an immunotherapeutic agent.

Finally, the DOX-loaded AcFu nanoparticles showed another interesting characteristic: they inhibited the drug efflux pump on the MDR cancer cell membranes. It is well known that MDR is still a significant hurdle in development of drug delivery systems (Parhi, Mohanty, & Sahoo, 2012). Surprisingly, in our FACS data (Fig. 6A–D) and confocal microscope images (Fig. 6E) of the MDR model cells (HCT-8), uptake of DOX was clearly shown in the case of DOX-loaded AcFu nanoparticles but not in the cases of the fucoidan–DOX mixture or free DOX. The mechanism for these differences is still unknown. However, according to B. Schnürch et al. (Bernkop-Schnurch and Grabovac, 2006) and our data, fucoidan may inhibit the drug efflux pump slightly. Thus, inhibition of the efflux pump by the DOX-loaded AcFu nanoparticles may be caused by interactions between AcFu and efflux protein. On the basis of structural difference between natural fucoidan and AcFu, the hydrophobicity of AcFu may increase the binding affinity to cell membrane-inserted drug efflux protein. Similar cellular uptake efficiencies for DOX were shown for all three cases for the non-MDR cancer cell line

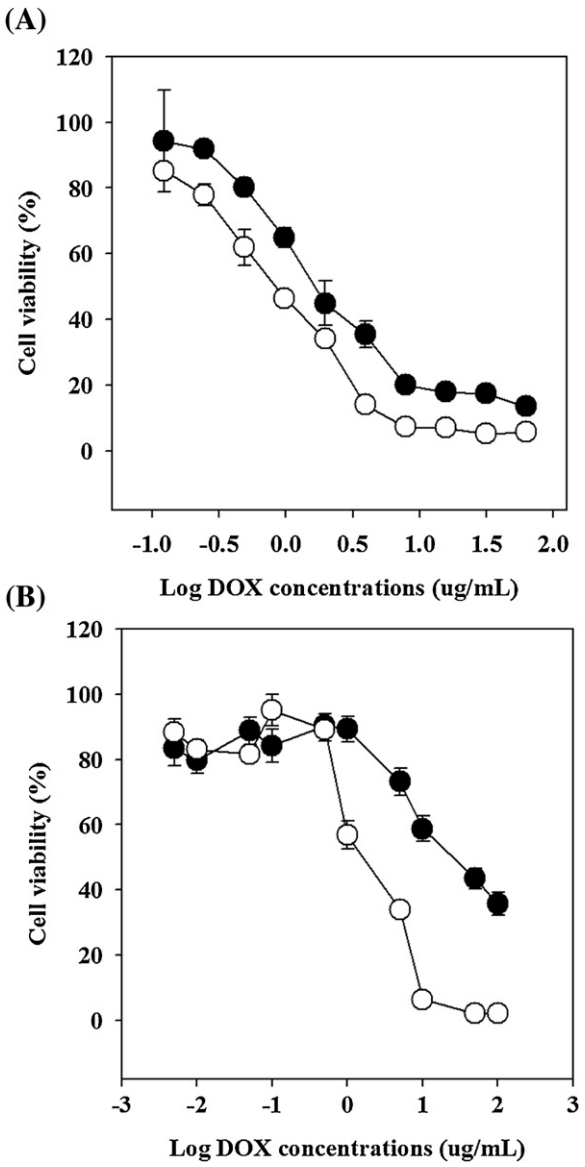

Fig. 7. Cytotoxicity of DOX-loaded nanoparticles. Similar cytotoxicity of AcFu nanoparticles (○) was shown in (A) HCT-116 and (B) HCT-8 cells whereas differences were observed for free DOX (●).

(HCT-116). Therefore, in the HCT-8 cells, the cytotoxicity of the DOX loaded AcFu nanoparticles was 23.9 times lower than that of free DOX (Fig. 7B), whereas similar IC_{50} values were observed for the two DOX preparations in the HCT-116 cells (Fig. 7A) due to the different cellular uptake efficiencies in the MDR cells.

Immuno- and chemotherapeutic efficiencies of the AcFu nanoparticles were confirmed separately, but these particles have significant advantages such as first-order drug release, immunomodulation and drug efflux pump inhibition. We therefore suggest that AcFu nanoparticles have a promising potential to be developed as a single-step immuno-chemotherapy system, and the immuno-chemotherapeutic efficiency of AcFu nanoparticles should be further examined in vivo.

5. Conclusion

To develop an immuno-chemotherapeutic system, DOX-loaded AcFu nanoparticles were investigated. The nanoparticles were formed via a dialysis method. The loaded drug was released via first order kinetic. AcFu has important functions, such as immunomodulation and drug efflux pump inhibition. Therefore, we suggest that AcFu nanoparticles have a promising potential for development as a one-step immuno-chemotherapeutic system.

Acknowledgment

This research was financially supported by the Korean Ministry of Education, Science and Technology through Strategic Research (2011-0028726).

Appendix A. Supplementary data

Supplementary data associated with this article can be found, in the online version, at http://dx.doi.org/10.1016/j.carbpol.2013.02.018.

References

Aisa, Y., Miyakawa, Y., Nakazato, T., Shibata, H., Saito, K., Ikeda, Y., et al. (2005). Fucoidan induces apoptosis of human HS-Sultan cells accompanied by activation of caspase-3 and down-regulation of ERK Pathways. *American Journal of Hematology*, *78*(1), 7–14.

Baxevanis, C. N., Voutsas, I. F., Tsitsilonis, O. E., Tsiatas, M. L., Gritzapis, A. D., & Papamichail, M. (2000). Compromised anti-tumor responses in tumor necrosis factor-α knockout mice. *European Journal of Immunology*, *30*(7), 1957–1966.

Bernkop-Schnurch, A., & Grabovac, V. (2006). Polymeric efflux pump inhibitors in oral drug delivery. *American Journal of Drug Delivery*, *4*(4), 263–272.

Chen, L., Lee, M. J., Li, H., & Yang, C. S. (1997). Absorption, distribution, and elimination of tea polyphenols in rats. *Drug Metabolism and Disposition*, *25*(9), 1045–1050.

Choi, E. M., Kim, A. J., Kim, Y. O., & Hwang, J. K. (2005). Immunomodulating activity of arabinogalactan and fucoidan in vitro. *Journal of Medicinal Food*, *8*(4), 446–453.

Grochow, L. B., Jones, R. J., Brundrett, R. B., Braine, H. G., Chen, T. L., Saral, R., et al. (1989). Pharmacokinetics of busulfan: Correlation with veno-occlusive disease in patients undergoing bone marrow transplantation. *Cancer Chemotherapy and Pharmacology*, *25*(1), 55–61.

Jeong, D., Seo, S., & Na, K. (2012). Drug stabilization and controlled release from AB 3 type tetra block copolymer based polymersome. *Journal of Pharmaceutical Investigation*, *42*(2), 101–108.

Kim, S. Y., Shin, I., Lee, Y. M., Cho, C. S., & Sung, Y. K. (1998). Methoxy poly (ethylene glycol) and-caprolactone amphiphilic block copolymeric micelle containing indomethacin. II. Micelle formation and drug release behaviours. *Journal of Controlled Release*, *51*(1), 13–22.

Lake, R. A., & Robinson, B. W. S. (2005). Immunotherapy and chemotherapy—A practical partnership. *Nature Reviews Cancer*, *5*(5), 397–405.

Li, F., Bae, B., & Na, K. (2010). Acetylated hyaluronic acid/photosensitizer conjugate for the preparation of nanogels with controllable phototoxicity: Synthesis, characterization, autophotoquenching properties, and in vitro phototoxicity against HeLa cells. *Bioconjugate Chemistry*, *21*(7), 1312–1320.

Manna, P. P., & Mohanakumar, T. (2002). Human dendritic cell mediated cytotoxicity against breast carcinoma cells in vitro. *Journal of Leukocyte Biology*, *72*(2), 312–320.

Maruyama, H., Tamauchi, H., Hashimoto, M., & Nakano, T. (2003). Antitumor activity and immune response of Mekabu fucoidan extracted from Sporophyll of Undariapinnatifida. *In Vivo (Athens Greece)*, *17*(3), 245.

Parhi, P., Mohanty, C., & Sahoo, S. K. (2012). Nanotechnology-based combinational drug delivery: An emerging approach for cancer therapy. *Drug Discovery Today*, *17*(17/18), 1044–1052.

Park, W., Park, S., & Na, K. (2010). Potential of self-organizing nanogel with acetylated chondroitin sulfate as an anti-cancer drug carrier. *Colloids and Surfaces B: Biointerfaces*, *79*(2), 501–508.

Park, W., Kim, K. S., Bae, B., Kim, Y., & Na, K. (2010). Cancer cell specific targeting of nanogels from acetylated hyaluronic acid with low molecular weight. *European Journal of Pharmaceutical Sciences*, *40*(4), 367–375.

Perales, M. A., Blachere, N. E., Engelhorn, M. E., Ferrone, C. R., Gold, J. S., Gregor, P. D., et al. (2002). Strategies to overcome immune ignorance and tolerance. *Seminars in Cancer Biology*, *12*, 63–71.

Rosenberg, S. A., Yang, J. C., & Restifo, N. P. (2004). Cancer immunotherapy: Moving beyond current vaccines. *Nature Medicine*, *10*(9), 909–915.

van der Most, R. G., Robinson, B. W. S., & Lake, R. A. (2009). Combining immunotherapy with chemotherapy to treat cancer. *Discovery Medicine*, *5*(27), 265–270.

Wagner, A. D., Grothe, W., Haerting, J., Kleber, G., Grothey, A., & Fleig, W. E. (2006). Chemotherapy in advanced gastric cancer: A systematic review and meta-analysis based on aggregate data. *Journal of Clinical Oncology*, *24*(18), 2903–2909.

Waterston, A., & Bower, M. (2004). TNF and cancer: Good or bad. *Cancer Therapy*, *2*, 131–148.

Yang, M., Ma, C., Sun, J., Shao, Q., Gao, W., Zhang, Y., et al. (2008). Fucoidan stimulation induces a functional maturation of human monocyte-derived dendritic cells. *International Immunopharmacology*, *8*(13), 1754–1760.